The Umbra and the Penumbra: Longitudinal Effects of Geographic Atrophy in AMD on the Outer Choroid by Imaging Analysis and Histopathological Correlation

Enrico Borrelli,[1,2] Francesco Cappellani,[3,4] Jose S. Pulido,[3,4] Daniel Pauleikhoff,[5] Imran A. Bhutto,[6] D. Scott McLeod,[6] Michele Reibaldi,[1,2] and Malia M. Edwards[6]

[1]Department of Surgical Sciences, University of Turin, Turin, Italy
[2]Department of Ophthalmology, "City of Health and Science" Hospital, Turin, Italy
[3]Vickie and Jack Farber Vision Research Center, Wills Eye Hospital, Philadelphia, Pennsylvania, United States
[4]Retina Service, Wills Eye Hospital, Philadelphia, Pennsylvania, United States
[5]St. Franziskus Hospital, Münster, Germany
[6]Ophthalmology, Wilmer Eye Institute, The Johns Hopkins University School of Medicine, Baltimore, Maryland, United States

Correspondence: Enrico Borrelli, Division of Ophthalmology, Department of Surgical Sciences, University of Turin, Via Cherasco, Turin 23, Italy; borrelli.enrico@yahoo.com.

Received: April 23, 2024
Accepted: November 2, 2024
Published: December 2, 2024

Citation: Borrelli E, Cappellani F, Pulido JS, et al. The umbra and the penumbra: Longitudinal effects of geographic atrophy in AMD on the outer choroid by imaging analysis and histopathological correlation. *Invest Ophthalmol Vis Sci.* 2024;65(14):2. https://doi.org/10.1167/iovs.65.14.2

Purpose. To quantitate regional changes in the outer choroidal vessels in patients with geographic atrophy (GA) in AMD and to correlate with a histopathological donor sample.

Methods. We analyzed 35 participants with GA for in vivo analysis and 1 participant with subject for histopathological analysis. Participants underwent three structural optical coherence tomography scans spaced 6 months apart over 1 year. Quantitative measurements of the outer choroidal vessels were performed in three regions: the GA region, a 150-µm-wide border surrounding the GA, and the area beyond the border. Histopathological analysis was performed using europaeus agglutinin lectin–stained choroidal flat-mount images with the focal planes of both the choriocapillaris and the outer choroidal vessels.

Results. In the GA region, the median vessel area was 3390 µm^2 (interquartile range [IQR], 2821 µm^2) at baseline, 3139 µm^2 (IQR, 2888 µm^2) at the 6-month visit and 2888 µm^2 (IQR, 2617 µm^2) at the 12 month visit ($P < 0.001$). Our cohort was divided into two subgroups based on RPE atrophy development at the GA border at the 6-month visit. This analysis showed that significant choroidal shrinking occurred only in eyes where the GA border progressed to GA at the 6-month follow-up. Histopathological analysis also demonstrated loss of the outer choroidal vessels, which were predominant in the GA region.

Conclusions. The outer choroidal vessels seem to decrease with time within the area of GA. The outer vessels decrease over time in eyes where the GA progresses. This finding may suggest that these vessels are under a very tight paracrine control.

Keywords: age-related macular degeneration, choroid, optical coherence tomography

AMD is a major cause of vision loss in the elderly, with geographic atrophy (GA) representing a severe late-stage manifestation of the disease.[1,2] Although the exact mechanisms driving GA remain incompletely understood, ongoing research suggests that the development and progression of GA may be influenced by a combination of factors, including oxidative stress, environmental influences, and genetic predisposition.[3,4] Changes in the choroid represent an important biomarker of AMD and the development and progression of GA.[5–8] Consequently, advancements in imaging technologies have played a crucial role in enhancing our understanding of choroidal changes in AMD and GA by improving our ability to study and characterize the choroid.[9]

Optical coherence tomography angiography (OCTA) has provided detailed visualization of the choriocapillaris (CC), enabling quantification of perfusion in this layer.[9] Studies using OCTA in eyes with early or intermediate AMD have shown that the CC is affected in these eyes,[10,11] corroborating findings from previous histopathological studies.[12–14] Importantly, OCTA studies have revealed significant alterations in the CC in eyes with GA, with notable spatial variations.[15–17] The CC was found to be affected more profoundly in the region of GA and less prominently affected at the border of GA, as also suggested by histopathological data.[6–8] Moreover, less CC perfusion at the border of GA was associated with faster longitudinal growth of GA over time.[15–17]

Advancements such as enhanced depth imaging and swept source technologies have improved the capability of structural OCT to assess outer choroidal vessels substantially.[18] Several investigations have focused on choroidal thickness in patients with GA and have shown significant

thinning consistently compared with age-matched healthy controls.[19,20] These findings have provided support that not only is the CC affected in GA, as discussed elsewhere in this article, but also that the outer choroidal vessels might be impacted as well, although this finding has not been well-documented either histologically or by imaging in vivo.

An intrinsic limitation in assessing choroidal thickness is its inability to provide spatial information regarding alterations in outer choroidal vessels. Performing a topographical evaluation of choroidal thickness may not be entirely fair owing to existing physiological variations, where thickness is typically higher in the foveal region and decreases gradually toward the periphery. Likewise, the dimensions of outer choroidal vessels vary depending on their topographic location beneath the macula. Nevertheless, it remains crucial to comprehend the impact of GA on outer choroidal vessels, especially concerning their distribution across different regions, including the GA lesion itself, its border, and the surrounding area. Given that previous studies have clarified the connection between the CC and the RPE,[10–14] investigating the outer choroidal vessels in GA would offer valuable insights into how the RPE interacts with the choroid in the context of GA.

The main aim of this study was to explore longitudinally regional quantitative differences in the outer choroidal vessels of patients affected by GA. Additionally, we evaluated and compared the OCT findings to the histopathological findings in the deeper choroidal vessels in a donor eye with GA.

Methods

Study Participants in the In Vivo Analysis

This retrospective cohort study was approved by the University of Turin Committee, following the guidelines of the 1964 Helsinki declaration and its subsequent revisions. Prior informed consent was obtained from all participants involved in the study.

Patients with GA secondary to AMD were identified from the medical records of the Medical Retina Unit at the City of Health and Science Hospital at the University of Turin. The diagnosis of GA was confirmed through a comprehensive assessment involving fundus ophthalmoscopy, fundus autofluorescence, and structural OCT. Specifically, GA was diagnosed when a hypopigmented area with visible choroidal vessels on fundus ophthalmoscopy corresponded with a hypoautofluorescent area on fundus autofluorescence, along with associated RPE atrophy visualized on structural OCT, as previously described.[21]

During the baseline visit, the following exclusion criteria were applied to the study eye: (i) previous history or evidence of macular neovascularization, including nonexudative cases; (ii) prior complex cataract or vitreoretinal surgeries including anti-VEGF injections; and (iii) a history or evidence of other retinal and optic nerve disorders. Additionally, participants were required to not develop macular neovascularization throughout the 1-year follow-up period and to have at least three retinal visits, including structural OCT assessments, covering a span of 12 months from the baseline visit. This choice was made to ensure three visits for evaluating outer choroidal vessels, occurring at the baseline, 6-month, and 12-month follow-up visits.

Structural OCT imaging was conducted using the Heidelberg Spectralis HRA+OCT device (Heidelberg Engineering, Heidelberg, Germany). The spectral domain OCT imaging session comprised six radial linear B-scans captured with enhanced depth imaging and centered on the fovea. Each B-scan (size X, 1536 pixels in length, approximately 8.5 mm; size Z, 496 pixels in length, approximately 1.9 mm) consisted of 25 averaged OCT images. A minimum signal strength of 25 was required for OCT images to be included, as per the manufacturer's recommendation.[22] Images acquired during different visits were taken using an eye-tracking–based follow-up function, which ensures that subsequent images are captured from the same retinal position as the baseline image. This system tracks near-infrared images of the retina to maintain consistent scanning of the same retinal location, thereby ensuring reliable assessment and measurement of the choroidal region over time.

OCT Grading

Initially, baseline and follow-up structural OCT images underwent eligibility review by an experienced and certified grader (E.B.). Subsequently, qualified eyes were independently assessed for quantitative metrics by another grader (F.C.). Specifically, baseline and follow-up structural OCT images centered on the fovea were exported in PNG format and then imported into ImageJ software version 2.0 (National Institutes of Health, Bethesda, MD; accessible at http://rsb.info.nih.gov/ij/index.html) for image analysis.

Quantitative measurements of the outer choroidal vessels were made in one of the 6 radial linear B-scans centered on the fovea and conducted in three distinct regions: (i) the GA region, (ii) a 150-µm-wide border surrounding the GA, and (iii) the area beyond the border. The OCT scan was selected at baseline, and the image clearly displaying the three distinct areas was chosen. When multiple images were available, the selection was made casually. The same image was evaluated subsequently during follow-up visits. In the GA region, all identifiable outer choroidal vessels (defined by an oval shape with hyper-reflective margins and hyporeflective contents), irrespective of whether they belonged to the Sattler's or Haller's layer, were selected. Along the ring surrounding the GA border, the first visible outer choroidal vessel moving outward from the GA region was chosen and measured. In the area beyond the border region, the first visible outer choroidal vessel from the outer edge of the ring was identified and analyzed (Fig. 1). In total, 113 choroidal vessels were identified at baseline and tracked through subsequent follow-up visits. Specifically, 43 choroidal vessels were identified within the GA region, 35 choroidal vessels were assessed in the 150-µm-wide border surrounding the GA, and another 35 choroidal vessels were evaluated in the area beyond the border. For each vessel, measurements of the area, along with the horizontal and vertical diameters separately, were recorded during each visit. Before beginning the measurements, the grader identified the orientation of the vessel, and measurements of vertical and horizontal diameters were taken in accordance with the vessel's orientation (i.e., the vertical diameter aligned with the vessel's vertical orientation) (Fig. 2).

The grader remained masked to the patient's identity and the timepoint of follow-up, and all images were mixed and graded randomly. The grader was provided

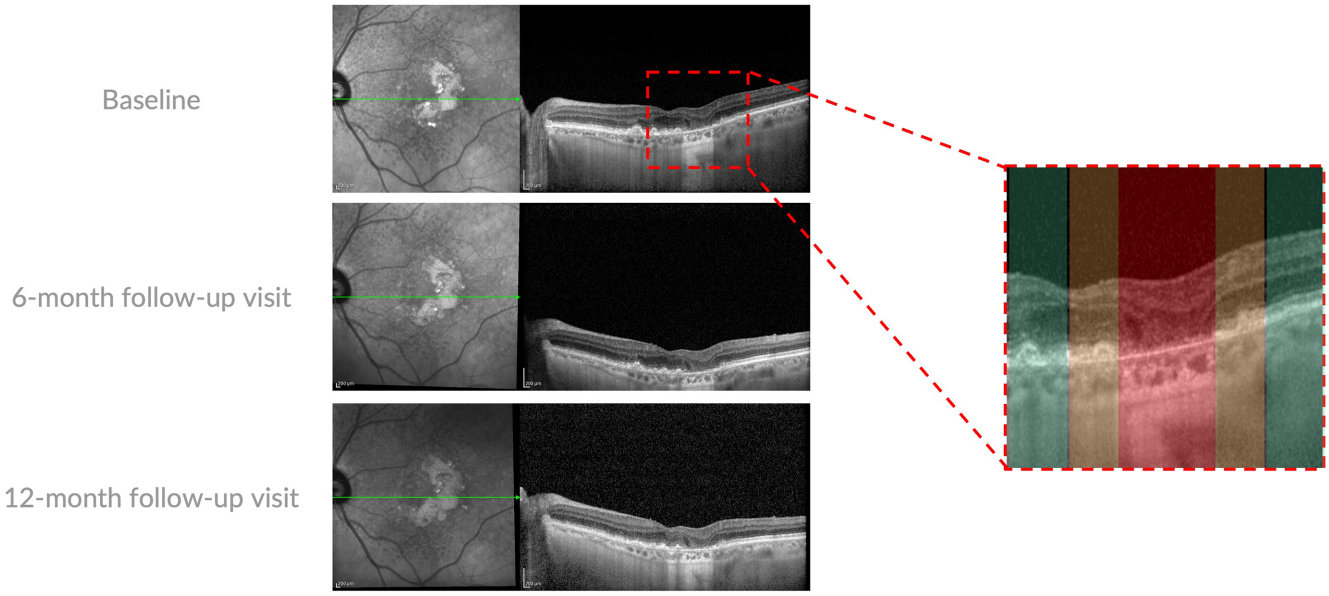

Figure 1. Representative OCT B-scans of a patient with GA. Enhanced depth imaging OCT B-scan (left) through the fovea were investigated at the baseline, 6-month, and 12-month follow-up visits. A magnified visualization of the investigated area is reported on the *right*. In detail, three regions were investigated: (i) GA region (highlighted in red), (ii) a 150-µm-wide border around the GA (highlighted in orange), and (iii) an area beyond the border (highlighted in green). In the GA region, all identifiable outer choroidal vessels (defined by oval shape with hyperreflective margins and hyporeflective contents) were selected and measured using ImageJ. Along the ring surrounding the GA border, the first visible vessel moving outward from the GA region was chosen and measured. In the area beyond the border region, the first visible vessel from the outer edge of the ring was identified and analyzed.

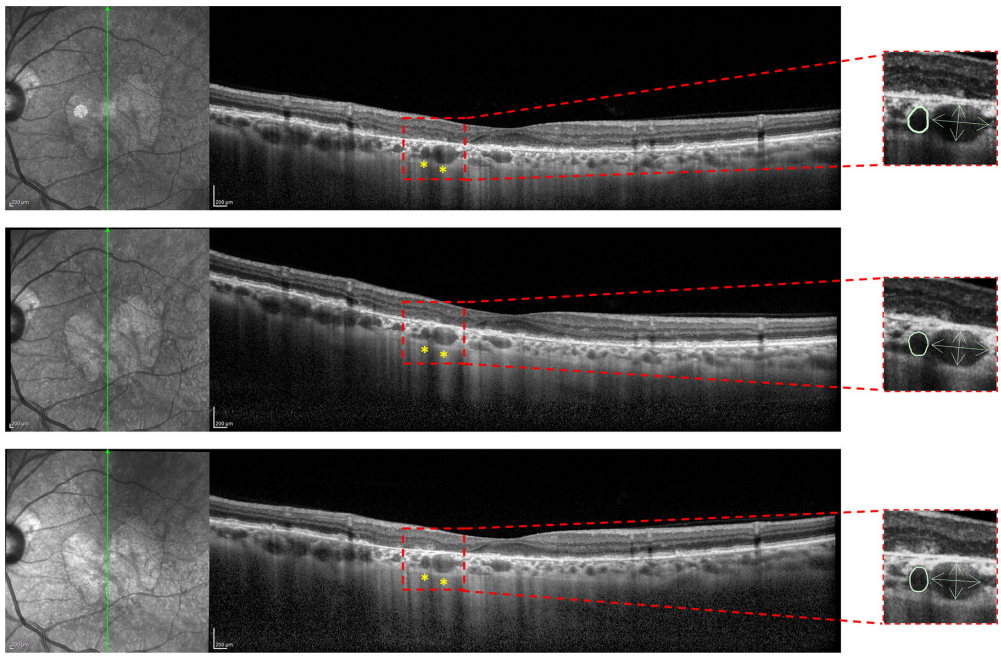

Figure 2. Example of the grading made to obtain OCT metrics of the choroidal vessels. For each patient, choroidal vessels were identified in the three regions of interest. In this particular case, two choroidal vessels were found within the GA area at baseline and were monitored throughout the follow-up visits. As shown on the *right side* of the image, measurements were taken for each vessel, including the area, as well as the horizontal and vertical diameters separately, at each visit. Before starting the measurements, the grader determined the vessel's orientation, ensuring that the vertical and horizontal diameters were measured in alignment with the vessel's respective orientation (i.e., the vertical diameter aligned with the vertical orientation of the vessel).

Investigative Ophthalmology & Visual Science

with highlighted arrows on the vessels to be measured, ensuring clarity regarding which vessels needed to be measured. To ensure effective blinding, grading tasks were also carried out on separate days. Grading outcomes were exported as a binary mask and automatically quantified in μm^2 and µm.

On structural OCT, untransformed GA area was graded to be present when a complete RPE and outer retinal atrophy (cRORA) was detected.[23] The CAM group defined cRORA as an area characterized by hypertransmission spanning at least 250 µm in diameter, accompanied by a zone of RPE attenuation or disruption of at least 250 µm in diameter, along with evident photoreceptor degeneration. The borders of the cRORA regions detected on structural OCT B-scans were annotated on the corresponding near infrared image taken simultaneously with the structural OCT scans.

Donor Eye and Tissue Preparation for Histopathological Analysis

A 90-year-old human donor eye affected by GA was obtained from a Caucasian individual, with the donation being prearranged directly with the donor's family. Eyes were received 24 hours postmortem, following shipment on wet ice. The use of this human tissue adhered to the principles outlined in the Declaration of Helsinki and was approved by the Joint Committee on Clinical Investigation at the Johns Hopkins University School of Medicine.

The whole globes were opened at the limbus, and the anterior segments were removed, leaving the posterior eyecups for microscopic examination using a Zeiss Stemi 2000-C Stereo Microscope (Carl Zeiss, Inc., Jena, Germany). Digital images of the eyecups were captured using a Gryphax NAOS 20 Megapixel Full HD USB 3.0 Color Digital Microscope Camera (Jenoptik, Rochester Hills, MI, USA) with both reflected and transmitted illumination before dissection. The retina and vitreous were removed and eyecups containing the choroid with intact RPE were reimaged. This allowed for visualization of the atrophic area. The eyecup was then immersed in 1% EDTA (disodium salt; dihydrate crystal; Baker Chemical Co., Radnor, PA, USA) in distilled water for 2 hours at room temperature. This process facilitated the removal of the RPE. Any remaining RPE cells were eliminated by pipetting the choroid with EDTA solution using a syringe with a blunted 25G needle. Gross digital images of choroids were then captured without RPE. Subsequently, RPE-denuded choroids were dissected from the sclera, briefly washed in 0.1 M cacodylate, and fixed overnight in 2% paraformaldehye in 0.1 M cacodylate buffer at 4°C.

The choroid was stained using immunohistochemistry following previously established protocols.[7,8,24] Briefly, the fixed tissue was washed and then blocked using 5% normal goat serum prepared in Tris-buffered saline with 0.1% bovine serum albumin and 1% Triton X-100. Subsequently, the tissue was incubated in a primary antibody cocktail for 72 hours, followed by washing in Tris-buffered saline with Tween three times and incubation in a secondary antibody cocktail for 48 hours. Ulex europaeus agglutinin (UEA) lectin/FITC conjugate (1:100, cat. GTX01512; GeneTex, Inc., Irvine, CA, USA) was included in the secondary antibody cocktail for vascular labeling. All blocking, antibody incubations, and washes were performed at 4°C. The choroid was then imaged using a Zeiss LSM 710 confocal microscope (Carl Zeiss Microscopy, LLC, Thornwood, NY, USA) and analyzed with Zen software. For the purpose of this paper, only the UEA lectin staining is shown. *Z*-stack images were collected from the UEA-stained choroidal flat-mounts. The focal planes at the level of the CC and outer choroidal vessels were assessed.

Statistical Analysis

All quantitative variables were reported as mean, median, SD, and interquartile range (IQR) in the Results and in the tables. The data distribution was not normal, as confirmed by the Shapiro–Wilk test ($P < 0.05$). Visual inspections using histograms and Q–Q plots also indicated deviations from normality. We attempted several transformations (log, square root, box–Cox) to normalize the data; however, normality could not be adequately achieved (all $P < 0.05$). Consequently, we used the nonparametric Friedman test and Durbin–Conover pairwise comparisons to investigate choroidal changes. All statistical analyses were carried out with the Jamovi software (version 2.4.12.0), setting the threshold for statistical significance at 0.05.

Results

Characteristics of Patients Included in the In Vivo Analysis

A total of 35 eyes from 35 patients (23 females) with GA secondary to non-neovascular AMD were included in our analysis. The mean patient age was 74.7 ± 7.8 years (range, 69–91 years).

Overall, the BCVA was 0.19 ± 0.18 LogMAR (Snellen VA of approximately 20/32) at baseline and 0.23 ± 0.20 LogMAR (Snellen VA of approximately 20/32) at the 12-month follow-up visit. The untransformed GA area size was 2.75 ± 1.74 mm^2 at baseline and 3.24 ± 2.25 mm^2 at the 12-month follow-up visit.

Our cohort was divided into two subgroups according to the status of the GA border at the 6-month follow-up visit, yielding a group of 12 cases where the GA border exhibited no RPE atrophy at baseline but progressed into GA at the 6-month follow-up and 23 cases where the border did not transition into GA during the follow-up period. The GA border was assessed for cRORA involvement at the 6-month follow-up visit. Specifically, in the direction where the vessel was selected and measured at baseline, it was graded as affected by atrophy when this region showed signs of cRORA at the follow-up visit.

Outer Choroidal Vascular Changes Considering the Whole Study Cohort in the In Vivo Analysis

Table 1 and Figure 3 summarize the longitudinal choroidal vascular changes observed in the topographical analysis. In the GA region, the median vessel area was 3390 μm^2 (IQR, 2821 μm^2) at baseline, 3139 μm^2 (IQR, 2888 μm^2) at the 6-month follow-up visit, and 2888 μm^2 (IQR, 2617 μm^2) at the 12-month follow-up visit ($P < 0.001$). Similarly, there was a significant decrease observed in both horizontal and vertical vessel diameters from baseline (median, 51.7 µm and median, 84.5 µm; IQR, 26.7 and IQR,52.0

Investigative Ophthalmology & Visual Science

Table 1. Topographical Analysis of the Choroidal Vessels at the Different Visits

	Visits			
	Baseline	6-Month Follow-Up Visit	12-Month Follow-Up Visit	*P* Value
Choroidal vessels in the GA region ($n = 43$)				
Vessel area, mean (median; IQR; SD)	4348 (3390; 2821; 3290)	3831 (3139; 2888; 2970) <0.001*	3516 (2888; 2617; 2712) <0.001† 0.003‡	<0.001*
Vessel horizontal diameter, mean (median; IQR; SD)	53.6 (51.7; 26.7; 20.8)	50.4 (49.1; 30.2; 20.2) 0.004†	47.8 (48.7; 27.7; 17.3) <0.001† 0.521‡	0.002*
Vessel vertical diameter, mean (median; IQR; SD)	90.8 (84.5; 52.0; 42.6)	83.1 (80.4; 40.8; 39.0) 0.001†	79.5 (77.1; 41.1; 38.6) <0.001† 0.032‡	<0.001*
Choroidal vessels in the GA border ($n = 35$)				
Vessel area, mean (median; IQR; SD)	3233 (2367; 2283; 2543)	3091 (2260; 3170; 2457) 0.493†	2896 (2009; 2340; 2387) 0.015† 0.074‡	0.043*
Vessel horizontal diameter, mean (median; IQR; SD)	45.7 (37.5; 19.7; 23.6)	44.0 (39.4; 24.3; 20.9) 0.555†	42.2 (39.7; 23.5; 20.4) 0.516† 0.953‡	0.766*
Vessel vertical diameter, mean (median; IQR; SD)	78.3 (70.8; 43.0; 33.3)	74.8 (70.8; 45.9; 35.0) 0.029†	71.4 (72.3; 46.0; 34.7) 0.001† 0.281‡	0.006*
Choroidal vessels in the area beyond the border ($n = 35$)				
Vessel area, mean (median; IQR; SD)	4026 (3139; 3548; 2439)	3758 (3014; 2874; 2219) 0.151†	3510 (2763; 3026; 2145) <0.001† 0.028‡	0.003 *
Vessel horizontal diameter, mean (median; IQR; SD)	51.0 (48.3; 29.8; 22.5)	49.3 (45.0; 27.5; 18.6) 0.308†	47.2 (45.7; 24.9; 18.8) 0.096† 0.509‡	0.239*
Vessel vertical diameter, mean (median; IQR; SD)	89.9 (82.6; 42.5; 29.2)	85.8 (84.1; 27.2; 29.6) 0.430†	82.0 (78.3; 37.6; 29.9) <0.001† 0.002‡	<0.001*

IQR, interquartile range; SD, standard deviation.
P values were obtained with the Friedman test and Durbin–Conover pairwise comparisons.
* *P* value obtained with the Friedman test.
† P value for the pairwise comparison vs. baseline using the Durbin–Conover test.
‡ *P* value for the pairwise comparison vs. 6-month follow-up using the Durbin–Conover test.

µm, respectively) to the 6-month follow-up (median, 51.7 µm and median, 84.5 µm; IQR, 26.7 µm and IQR, 52.0 µm, respectively), and to the 12-month follow-up (median, 51.7 µm and median, 84.5 µm; IQR, 26.7 µm and IQR,52.0 µm, respectively) measurements ($P = 0.002$ and $P < 0.001$, respectively).

In the GA border, the median vessel area was 2367 µm^2 (IQR, 2283 µm^2) at baseline, showing a slight reduction over the follow-up period ($P = 0.043$). However, no statistically significant changes were observed after 6 months (median, 2260 µm^2; IQR, 3170 µm^2; $P = 0.493$), whereas these changes became statistically significant after 12 months (median, 2009 µm^2; IQR, 2340 µm^2; $P = 0.015$). In the area beyond the border, the median vessel area was 3139 µm^2 (IQR, 3548 µm^2) at baseline, showing a slight reduction throughout the follow-up ($P = 0.003$). Similar to the GA border, no statistically significant changes were detected after 6 months (median, 3014 µm^2; IQR, 2874 µm^2; $P = 0.151$), but significant changes were observed after 12 months (median, 2763 µm^2; IQR, 3026 µm^2; $P < 0.001$). Further details regarding vessel diameters in these two regions are provided in Table 1 and Figure 3.

In terms of vessel area, the average decrease after 6 months was 12.5% in the GA area, 6.8% in the GA border, and 3.2% in the area beyond the border. Likewise, the average reduction after 12 months was 19.6% in the GA area, 11.7% in the GA border, and 10.7% in the area beyond the border.

Investigative Ophthalmology & Visual Science

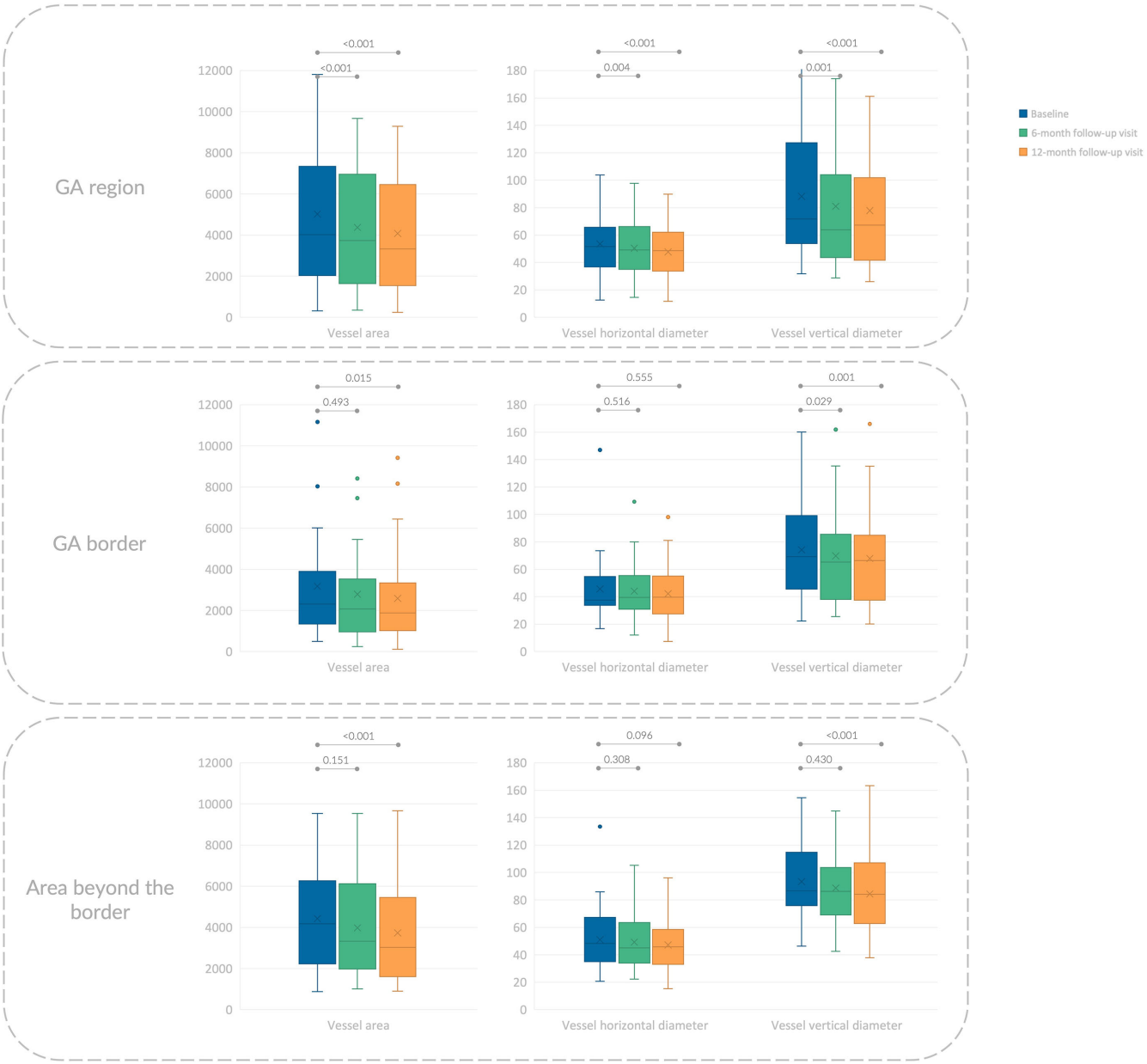

Figure 3. Box and whisker plots showing analyzed choroidal measurements in patients with GA. Each box indicates mean (*cross within the* box), median (*central horizontal line*), and IQR (*horizontal extremes of the box*) values for a specific variable at each visit. The minimum and maximum values correspond with the ends of the whiskers. *Dots* indicate outliers. On the *y* axis, values are reported in square micrometers and micrometers for area and diameters, respectively. The values at different visits are arranged along the *x* axis, with category labels provided in the legend in the *upper left corner*. Each row corresponds with a different region: (i) GA region (*top row*), (ii) 150-µm-wide border around the GA (*middle row*), and (iii) area beyond the border (*bottom row*). Further details on pairwise comparisons can be found in Table 1.

Outer Choroidal Vascular Changes Considering the Different Subgroups in the In Vivo Analysis

As stated elsewhere in this article, our cohort was split into two subgroups based on the condition of the GA border during the 6-month follow-up visit. This resulted in 12 cases where the GA border showed no signs of RPE atrophy at baseline, but progressed into GA at the 6-month follow-up and 23 cases where the border did not develop into GA during the follow-up period.

This subgroup analysis revealed that longitudinal choroidal changes in the GA border were only observed in eyes where the GA border progressed into GA at the 6-month follow-up (Table 2; Fig. 4). In this particular group, the median vessel area was 2040 µm^2 (IQR, 2741 µm^2) at baseline, decreasing to 1220 µm^2 (IQR, 3016 µm^2) at the 6-month follow-up visit, and further to 1294 µm^2 (IQR, 2688 µm^2) at the 12-month follow-up visit ($P < 0.001$). Conversely, no significant changes were observed in the GA border among patients where the border did not progress during the follow-up period (Table 2; Fig. 4).

Table 2. Choroidal Vessels in the GA Border in the Two Sub-Groups (Patients With Border Falling in the GA Area at the 6-Month Visit vs. Patients Without Border Falling in This Region)

	Visits			
	Baseline	6-Month Follow-Up Visit	12-Month Follow-Up Visit	*P* Value
Choroidal vessels in the GA border in patients with border falling into the GA (n = 12)				
Vessel area, mean (median; IQR; SD)	3110 (2040; 2741; 3033)	2401 (1220; 3016; 2441) 0.001†	1905 (1294; 2688; 1938) <0.001† 0.083‡	<0.001*
Vessel horizontal diameter, mean (median; IQR; SD)	49.0 (37.0; 24.6; 35.1)	39.9 (30.8; 32.8; 28.8) 0.049†	34.8 (31.1; 29.0; 24.7) 0.012† 0.500‡	0.039*
Vessel vertical diameter, mean (median; IQR; SD)	71.5 (64.1; 53.6; 29.2)	62.5 (51.8; 48.7; 33.6) 0.002†	56.3 (47.5; 52.1; 29.4) <0.001†	<0.001*
Choroidal vessels in the GA border in patients without border falling into the GA (n = 23)				
Vessel area, mean (median; IQR; SD)	3298 (2511; 2198; 2319)	3451 (2386; 2888; 2441) 0.334†	3412 (2135; 2825; 2473) 0.765† 0.208‡	0.407*
Vessel horizontal diameter, mean (median; IQR; SD)	44.0 (40.9; 17.1; 15.3)	46.2 (39.8; 21.0; 15.7) 0.561†	46.0 (40.2; 24.9; 17.0) 0.346† 0.716‡	0.623*
Vessel vertical diameter, mean (median; IQR; SD)	81.9 (72.6; 33.5; 35.4)	81.3 (79.3; 39.6; 34.6) 0.276†	79.3 (72.6; 35.0; 35.2) 0.382† 0.826‡	0.500*

P values were obtained with the Friedman test and Durbin–Conover pairwise comparisons.
* *P* value obtained with the Friedman test.
† *P* value for the pairwise comparison vs. baseline using the Durbin–Conover test.
‡ *P* value for the pairwise comparison vs. 6-month follow-up using the Durbin–Conover test.

Similar to the GA border, in the area beyond the border, longitudinal choroidal changes occurred only in those eyes where the GA border progressed to GA at the 6-month follow-up (Table 3; Fig. 4). In the latter group, the median vessel area was 4283 µm² (IQR, 3598 µm²) at baseline, 3655 µm² (IQR, 3438 µm²) at the 6-month follow-up visit, and 3223 µm² (IQR, 3309 µm²) at the 12-month follow-up visit ($P = 0.004$). Conversely, no significant modifications were detected in the area beyond the border in those patients where the border did not transition into GA during the follow-up period (Table 3; Fig. 4).

Histological Analysis

On gross observation (Figs. 5A, 5B), the donated eye with GA demonstrated RPE atrophy in the posterior pole. The atrophic area exhibited an oval shape with a clearly defined border, limited to the macular region. In this area, choroidal vessels were clearly visible. The UEA lectin-stained choroid clearly showed marked dropout of the CC in the atrophic area with only a few viable capillaries remaining (white arrows. Figs. 5C–E).[8] Microscopic examination of the choroidal flat-mount at the level of the outer choroidal vessels showed larger vessels were present and there were larger distances between vessels consistent with diminished vessel density (Figs. 5D, 6). At the border, the CC was patchy and there were outer choroidal vessels of larger and medium caliber with the distance between vessels appearing to be less than of the vessels in the GA area (Fig. 6, bottom middle image). Finally, in the area farther from the GA, the dense, freely interanastomosing pattern of normal CC was present, and the deeper choroidal vessels showed extensive medium sized and large deeper vessels (Fig. 6, bottom right image).

Discussion

In our study, we observed longitudinal modifications in the outer choroidal vessels among patients with AMD and GA. More importantly, we provided a topographical analysis of these outer choroidal changes to assess and measure these changes across three specific areas: (i) the GA region, (ii) the 150-µm-wide border around the GA, and (iii) the ring around the border. Our topographical analysis revealed a progressive diminishment in the size of outer choroidal vessels over time specifically within the GA region. Moreover, our cohort was divided into two subgroups according to the status of the GA border at the 6-month follow-up visit, yielding a group of 12 cases where the GA border exhibited no RPE atrophy at baseline but progressed into GA at the 6-month follow-up and 23 cases where the border did not transition into GA during the follow-up period. Interestingly, no longitudinal alterations in the size of outer choroidal vessels were observed in the GA border and the surrounding ring

Investigative Ophthalmology & Visual Science

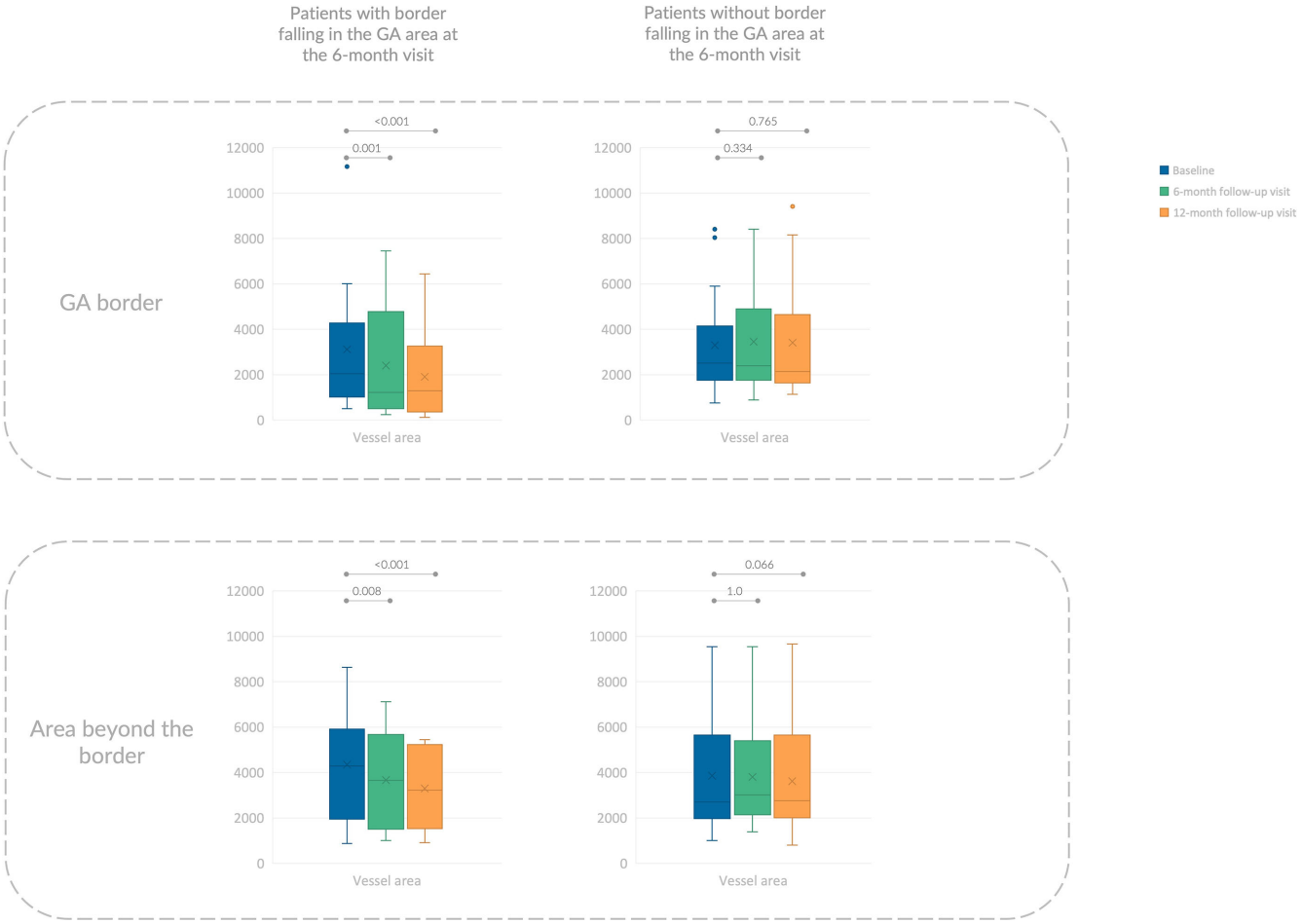

Figure 4. Box and whisker plots showing vessel area measurements in different subgroups of patients. Each box indicates mean (*cross within the box*), median (*central horizontal line*), and IQR (*horizontal extremes of the* box) values for a specific variable at each visit. The minimum and maximum values correspond to the ends of the whiskers. Dots indicate outliers. On the *y* axis, values are reported in square micrometers. The values at different visits are arranged along the *x* axis, with category labels provided in the legend in the upper left corner. Each row corresponds with a different region: (i) GA region (*top row*), (ii) 150-µm-wide border around the GA (*middle row*), and (iii) the area beyond the border (*bottom row*). Each column represents a different group: the *left column* displays values from the group where the GA border exhibited no RPE atrophy at baseline but progressed into GA at the 6-month follow-up, whereas the *right column* contains data from cases where the border did not transition into GA during the follow-up period. Additional details regarding pairwise comparisons can be found in Tables 2 and 3.

in patients where the border did not transition into GA during the follow-up period. Conversely, a notable decrease in vessel size was identified in these regions once the border progressed into GA at the 6-month follow-up. Taken together, these findings may suggest that outer choroidal changes predominantly impact areas exhibiting RPE atrophy. Nevertheless, alterations in the outer choroidal vessels beyond the border in eyes where the border transitions into the GA region may indicate early vascular changes possibly linked to a decrease in VEGF levels in the surrounding area.

We also presented a histopathological case that illustrates the CC and outer choroidal vessels in a patient with GA. This case seems to validate the intimate relationship of the choroidal vessels with the RPE and remarkably demonstrates that there is a substantial decrease in the size of the outer choroidal vessels, primarily coinciding with the region of RPE atrophy. These histological findings are thus in agreement with the earlier mentioned findings,[7,8,24] although the prior assessments were restricted in evaluating the CC. Consequently, because the CC was shown to be affected predominantly in the GA region in our case and previous reports, the outer choroidal vessels also seem to be impacted in this area.

The border of GA has garnered significant interest, because comprehending the alterations that affect the complex unit of photoreceptors, RPE cells, and choroid in this area could enhance our understanding of GA greatly. Using fundus autofluorescence, the border around GA typically shows regions of hyperautofluorescence. The latter finding is thought to be due to ongoing RPE cell dysfunction, vertically superimposed RPE cells, and variable photoreceptor loss.[25] Moreover, these alterations have demonstrated pathogenic significance: areas with increased autofluorescence may correlate with varying degrees of retinal sensitivity loss and precede the onset and expansion of GA.[26] The border of GA has also been extensively explored using structural OCT. Specifically, when the border is character-

Investigative Ophthalmology & Visual Science

Table 3. Choroidal Vessels Beyond the Border in the Two Subgroups (Patients With Border Falling in the GA Area at the 6-Month Visit vs. Patients Without Border Falling in This Region)

	Visits			
	Baseline	6-Month Follow-Up Visit	12-Month Follow-Up Visit	*P* Value
Choroidal vessels in the area beyond the border in patients with border falling into the GA (n = 12)				
Vessel area, mean (median; IQR; SD)	4351 (4283; 3598; 2384)	3666 (3655; 3438; 2129) 0.008†	3297 (3223; 3309; 1728) <0.001† 0.195‡	0.004
Vessel horizontal diameter, mean (median; IQR; SD)	58.1 (56.8; 28.9; 28.8)	51.1 (51.2; 29.2; 22.1) 0.049†	49.3 (48.4; 21.2; 18.8) 0.012† 0.500‡	0.017*
Vessel vertical diameter, mean (median; IQR; SD)	91.9 (85.9; 39.5; 26.6)	85.8 (86.0; 31.3; 28.5) 0.257†	81.4 (81.5; 29.7; 26.2) <0.001† 0.001‡	0.001*
Choroidal vessels in the area beyond the border in patients without border falling into the GA (n = 23)				
Vessel area, mean (median; IQR; SD)	3857 (2699; 2846; 2503)	3805 (3014; 2511; 2310) 1.0†	3622 (2763; 2604; 2362) 0.066† 0.066‡	0.107*
Vessel horizontal diameter, mean (median; IQR; SD)	47.2 (41.3; 25.5; 18.1)	48.3 (43.1; 26.6; 16.9) 0.718†	46.2 (45.7; 24.9; 19.2) 0.885† 0.613‡	0.867*
Vessel vertical diameter, mean (median; IQR; SD)	88.8 (82.6; 37.2; 31.0)	85.8 (79.3; 25.6; 30.8) 0.763†	82.4 (78.2; 39.6; 32.2) 0.055† 0.103‡	0.119*

P values were obtained with the Friedman test and Durbin-Conover pairwise comparisons.
* *P* value obtained with the Friedman test.
† *P* value for the pairwise comparison vs. baseline using the Durbin–Conover test.
‡ *P* value for the pairwise comparison vs. 6-month follow-up using the Durbin–Conover test.

ized by an augmented thickness of the RPE to Bruch's membrane layer,[27] a reduced thickness of the outer retinal layer,[28] and/or the presence of photoreceptor changes,[29] the progression of GA tends to be more rapid. Studies using OCTA have demonstrated that decreased perfusion in the CC at the border of GA is correlated with accelerated longitudinal expansion of GA over time.[15–17]

In alignment with retinal imaging studies aimed at better characterizing the border of GA, several histopathological investigations have also provided characterization of this region. In a previous study, Dolz-Marco et al.[3] showed that the RPE phenotype is irregular at the border of GA, demonstrating a higher presence of intraretinal migrated RPE cells. Furthermore, this region is distinguished by thicker and more extensive basal laminar deposits.[3]

Choroidal studies also offer insights.[7,8,24] McLeod et al.[24] analyzed postmortem choroids and found that despite RPE loss in GA, the CC can remain intact initially, suggesting RPE damage precedes CC degeneration. Seddon et al.[7] confirmed CC reduction in GA eyes, primarily in areas of RPE atrophy, with surviving vessels showing structural changes. Last, Edwards et al.[8] observed severe CC dropout in regions matching RPE atrophy, with constricted surviving vessels. Where RPE remained, the CC seemed to be similar to controls. These results support previous findings.

The mechanisms underlying our findings remain uncertain, but the observed decrease in outer choroidal vessel size could potentially be linked to decreased levels of VEGF owing to diminished production by the absent RPE (Fig. 7). The CC is known to rely heavily on growth factors, such as VEGF, secreted by the RPE.[30] Hence, the decreased number of CC vessels in the region of RPE atrophy, as detected by both in vivo imaging and histology, is not unexpected. Similarly, the longitudinal constriction of outer choroidal vessels observed in our study may be associated with atrophic RPE, resulting in decreased VEGF production and subsequent constriction of the outer choroidal vessels. Evidence suggests that VEGF may play a role in maintaining the health and tone of outer choroidal vessels. As an example, nitric oxide is involved in regulating choroidal blood flow through the outer choroidal vessels, and VEGF participates in nitric oxide signaling regulation.[31] Therefore, decreased VEGF production in regions with RPE atrophy could lead to reduced nitric oxide levels and subsequent longitudinal vasoconstriction of these vessels. One of the most significant observations from our study is that alterations in outer choroidal vessels occur specifically around the GA only when it enlarges in the direction where vessels were previously measured. This particular finding seems to reinforce the idea that there is a clear topographical relationship between the presence of the RPE and changes in the

Investigative Ophthalmology & Visual Science

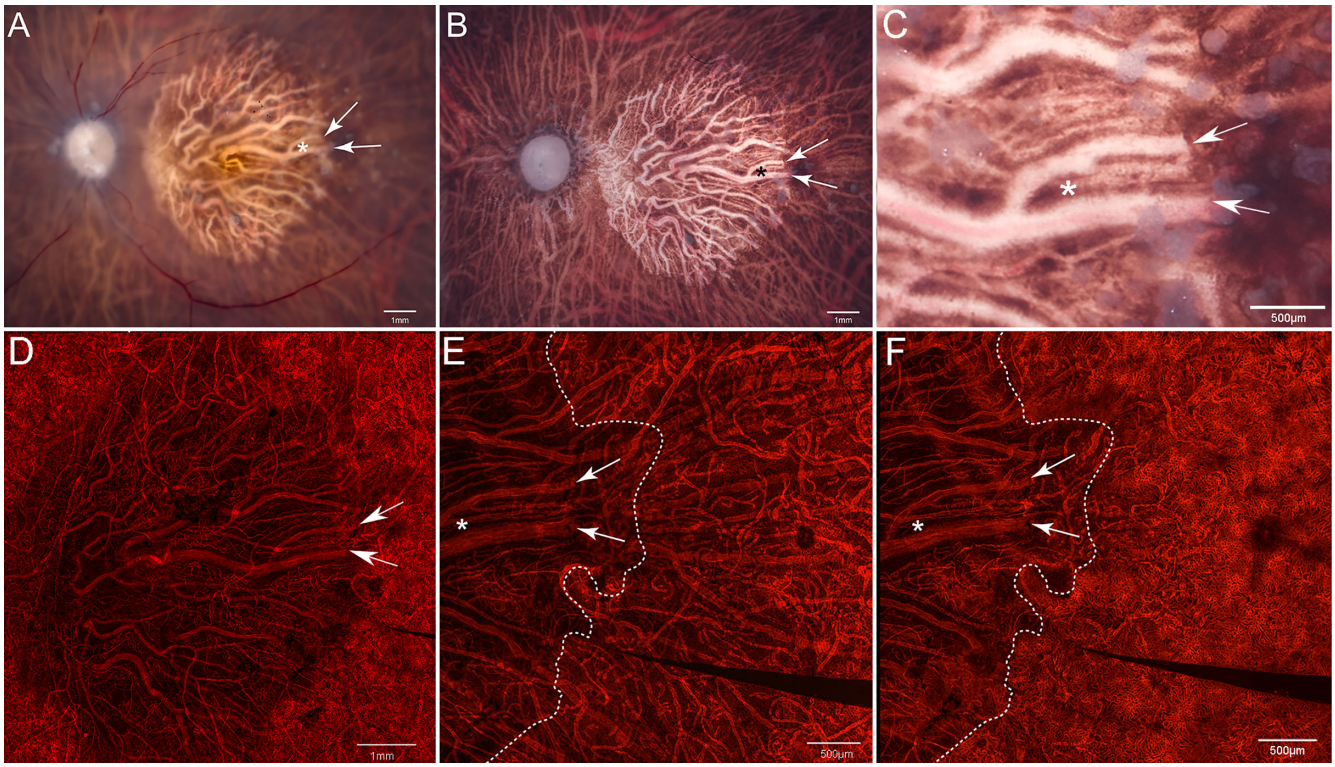

Figure 5. Gross photographs and choroidal flat-mounts. Gross photographs of the posterior eyecups from the donor with GA with retina intact (**A**) and postretinal dissection (**B**) reveal a significant area of RPE atrophy, indicated by white arrowheads, predominantly in the macular region (**C** offers a magnified visualization of this region). A low-magnification image of the choroidal flat-mount stained with UEA (**D**) demonstrates pronounced dropout of the CC within the area of RPE atrophy, as indicated by the *white arrowheads*. The high-magnification UEA-stained choroidal flat-mount image with the focal plane at the level of the outer choroidal vessels (**E**) illustrates fewer and thinner outer choroidal vessels in the region corresponding with RPE atrophy. Similarly, the high-magnification UEA-stained choroidal flat-mount image with the focal plane at the level of the CC vessels (**F**) depicts few viable capillaries within the CC, with blood vessels primarily composed of intermediate and large choroidal vessels within the GA area. Asterisks and arrows are used to denote the same structures in all images, whereas a dotted line delineates the border of the atrophic RPE.

outer choroidal vessels. Another explanation for our findings could be that primary CC vascular loss in regions affected by GA might result in constriction of outer vasculature owing to increased downstream resistance caused by the absence or constriction of CC vessels, as well as decreased blood return from these capillaries to the outer choroidal vessels. Further investigations are warranted to elucidate this relationship.

Our study has limitations, including the retrospective nature of the study. A prospective longitudinal evaluation of outer choroidal vessels in patients with GA may shed further light on the causal role of the RPE in choroidal changes. An important limitation is that we analyzed single outer choroidal vessels using structural OCT, rather than conducting a topographical analysis of the entire choroid. However, our objective was specifically to assess changes in the vascular component of the outer choroid, and we believed this approach was appropriate for this assessment. Moreover, we cannot exclude the possibility that our findings are related to physiological changes associated with aging rather than pathological modifications specifically related to AMD and GA. However, it is important to note that our observed changes were more pronounced in regions with RPE atrophy, which suggests a potential association with the pathogenesis of GA. Another notable limitation is the brief follow-up period of only 1 year. However, this duration is sufficient to evaluate significant changes while minimizing the influence of other factors, such as the progression of RPE atrophy, on the results. A key limitation of this study is that, although the eye-tracking system used allows for the evaluation of the same regions across multiple visits, it may not always capture the exact same retinal region during follow-ups owing to minor inaccuracies. Therefore, future volumetric assessments of the choroid could help further validate our findings. Strengths of our study include the use of enhanced depth imaging technology in all cases, which allowed precise analysis of outer choroidal changes over the follow-up period. More important, we provided histopathological data to further support our findings.

In summary, in this structural OCT study of the outer choroidal vessels, we observed that eyes with GA have longitudinal changes in these vessels mainly confined to regions with GA. Notably, we also examined the GA borders and found longitudinal thinning of the outer choroidal vessels only when RPE atrophy extended into these borders during follow-up. Histopathological findings in our study support the notion that outer choroidal changes predominantly occur in regions of RPE atrophy, indicating a potential tight paracrine control over these vessels. We anticipate that our findings will stimulate future prospective research to validate the sequential stages of outer choroidal modifi-

Investigative Ophthalmology & Visual Science

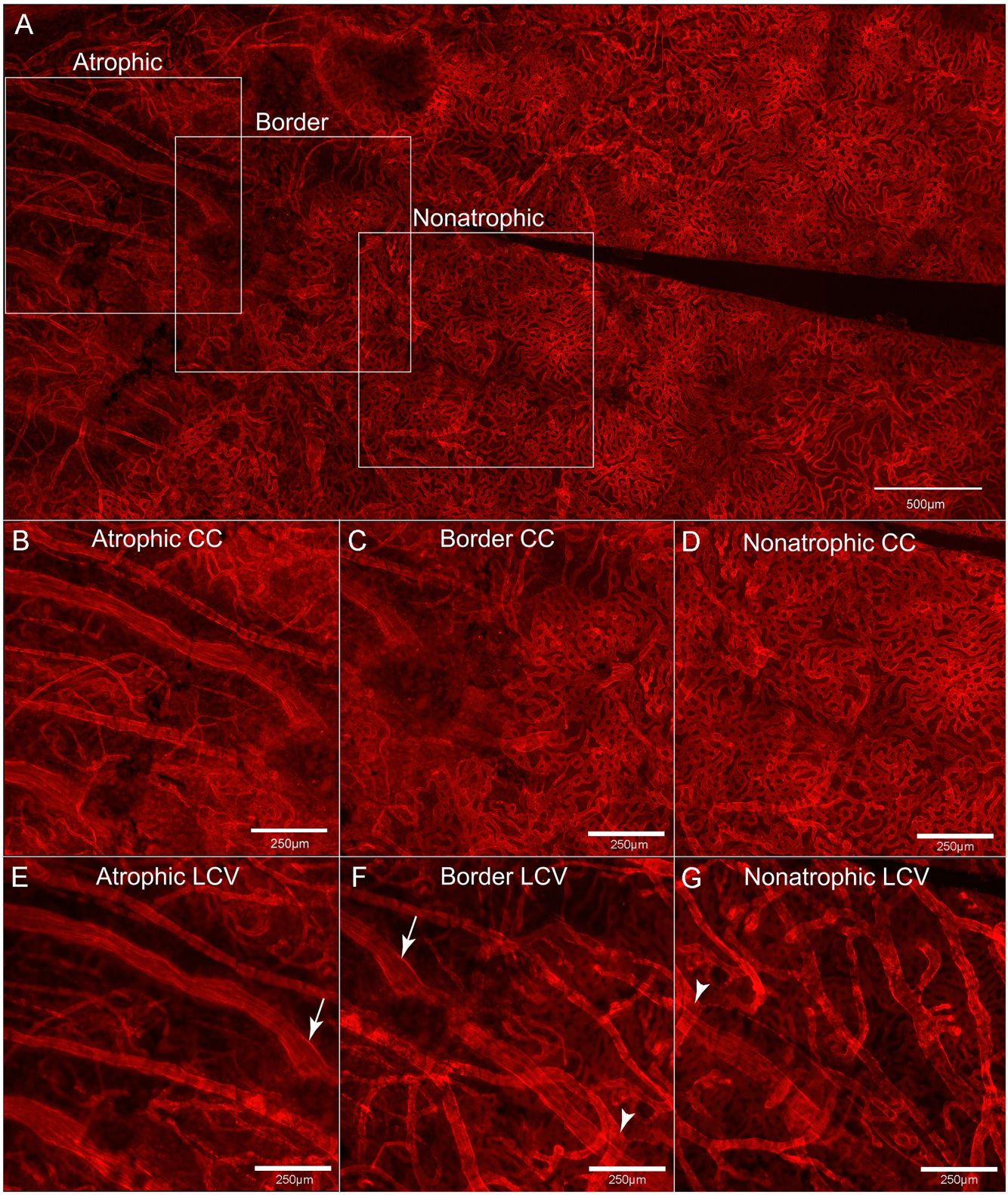

Figure 6. Low-magnification and representative high-magnification images of UEA-stained choroidal flat-mounts. The low-magnification image of the choroidal flat-mount stained with UEA (*top row*) highlights the locations where the subsequent high-magnification images are taken. The UEA-stained high-magnification choroidal flat-mount images, with the focal plane at the level of the CC (*middle row*) and outer choroidal vessels (*bottom row*), illustrate a trend of decreasing numbers and sizes of both CC and outer (i.e., or larger – LCV) choroidal vessels toward the region affected by RPE atrophy.

Investigative Ophthalmology & Visual Science

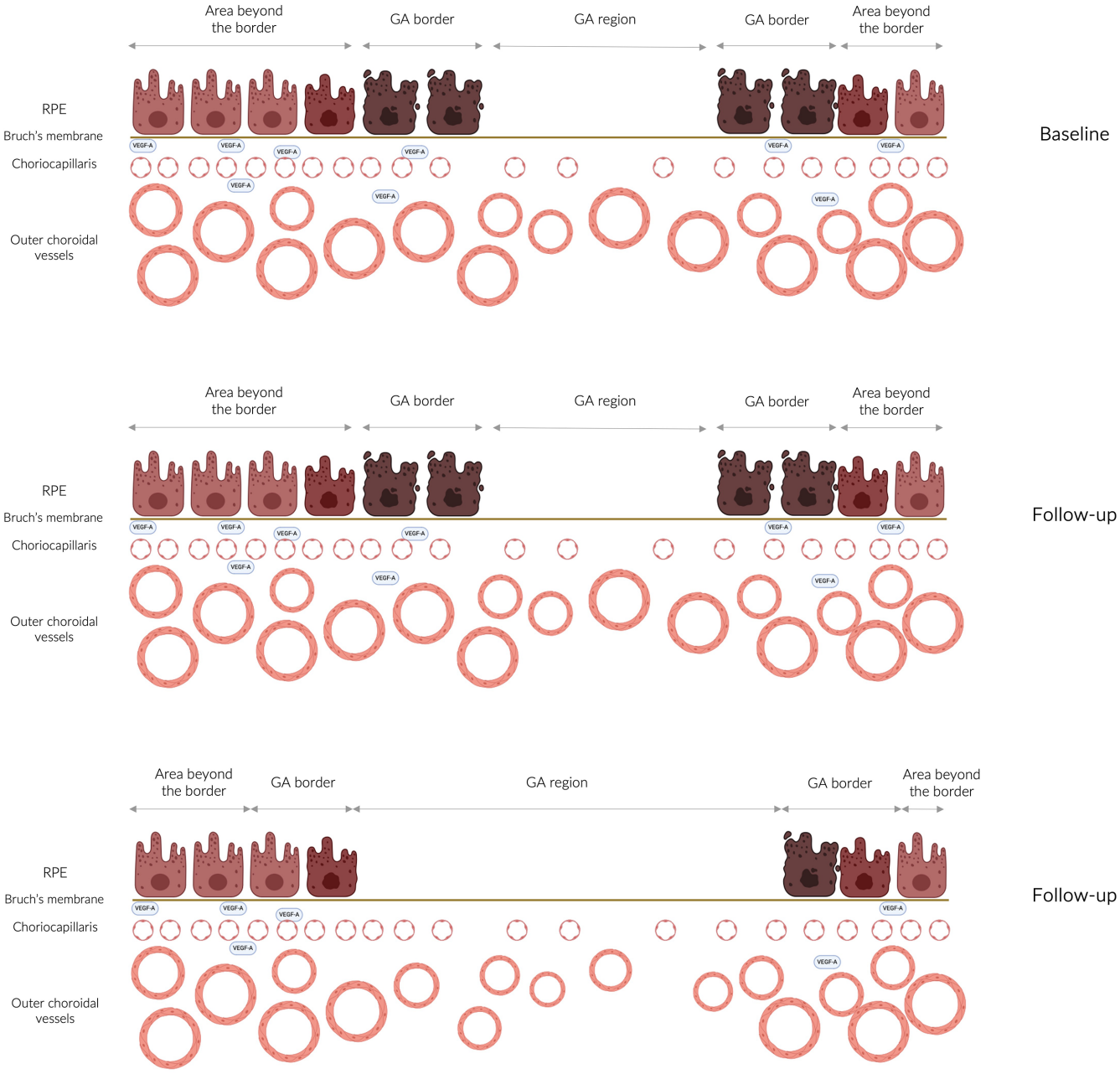

Figure 7. Cartoon diagrams illustrating the relationship between the RPE and choroidal vessels. Each row in the diagrams represents a different visit, with the top row representing the baseline assessment and the middle and bottom rows representing two follow-up visits. In the region with RPE atrophy, the outer choroidal vessels may decrease in size compared with the baseline assessment (*top row*) in the follow-up assessments (*middle and bottom rows*). This reduction may also extend to the border region if this area transitions into GA during the follow-up period (*bottom row*).

cations in GA. Moreover, additional clinicopathologic data are essential for a comprehensive understanding of outer choroidal vessel alterations, which could play a crucial role in GA's pathophysiology.

Acknowledgments

The authors thank the eye donor and his family for the generous gift to science.

Supported by NEI/NIH R01EY016151 (ME), & EY001765 (Wilmer P30 grant) and RPB unrestricted funds to Wilmer.

Disclosure: **E. Borrelli**, Abbvie (C), Bayer (C), Hofmann La Roche (C), Novartis (F), Zeiss (C); **F. Cappellani**, None; **J.S. Pulido**, None; **D. Pauleikhoff**, None; **I.A. Bhutto**, None; **D. Scott McLeod**, None; **M. Reibaldi**, Abbvie (C), Bayer (C), Hofmann La Roche (C), Novartis (C), Zeiss (C); **M.M. Edwards**, None

References

1. Ferris FL, Wilkinson CP, Bird A, et al. Clinical classification of age-related macular degeneration. *Ophthalmology*. 2013;120(4):844–851.

Investigative Ophthalmology & Visual Science

2. Klein R, Klein BEK, Linton KLP. Prevalence of age-related maculopathy: the Beaver Dam Eye Study. *Ophthalmology*. 2020;127(4S):S122–S132.
3. Dolz-Marco R, Balaratnasingam C, Messinger JD, et al. The border of macular atrophy in age-related macular degeneration: a clinicopathologic correlation. *Am J Ophthalmol*. 2018;193:166–177.
4. Fleckenstein M, Keenan TDL, Guymer RH, et al. Age-related macular degeneration. *Nat Rev Dis Primers*. 2021;7(1):31.
5. Bhutto I, Lutty G. Understanding age-related macular degeneration (AMD): relationships between the photoreceptor/retinal pigment epithelium/Bruch's membrane/choriocapillaris complex. *Mol Aspects Med*. 2012;33(4):295–317.
6. McLeod DS, Grebe R, Bhutto I, Merges C, Baba T, Lutty GA. Relationship between RPE and choriocapillaris in age-related macular degeneration. *Invest Ophthalmol Vis Sci*. 2009;50(10):4982–4991.
7. Seddon JM, McLeod DS, Bhutto IA, et al. Histopathological insights into choroidal vascular loss in clinically documented cases of age-related macular degeneration. *JAMA Ophthalmol*. 2016;134(11):1272–1280. Published online September 22, 2016.
8. Edwards MM, McLeod DS, Shen M, et al. Clinicopathologic findings in three siblings with geographic atrophy. *Invest Ophthalmol Vis Sci*. 2023;64(3):2.
9. Borrelli E, Sarraf D, Freund KB, Sadda SR. OCT angiography and evaluation of the choroid and choroidal vascular disorders. *Prog Retin Eye Res*. 2018;67:30–55. Published online 2018.
10. Borrelli E, Uji A, Sarraf D, Sadda SR. Alterations in the choriocapillaris in intermediate age-related macular degeneration. *Invest Ophthalmol Vis Sci*. 2017;(11):4792–4798.
11. Borrelli E, Shi Y, Uji A, et al. Topographical analysis of the choriocapillaris in intermediate age-related macular degeneration. *Am J Ophthalmol*. 2018;196:34–43.
12. Friedman E, Smith TR, Kuwabara T. Senile choroidal vascular patterns and drusen. *Arch Ophthalmol*. 1963;69:220–230.
13. Sarks SH, Arnold JJ, Killingsworth MC, Sarks JP. Early drusen formation in the normal and aging eye and their relation to age related maculopathy: a clinicopathological study. *Br J Ophthalmol*. 1999;83(3):358–368.
14. Mullins RF, Johnson MN, Faidley EA, Skeie JM, Huang J. Choriocapillaris vascular dropout related to density of drusen in human eyes with early age-related macular degeneration. *Invest Ophthalmol Vis Sci*. 2011;52(3):1606.
15. Nassisi M, Baghdasaryan E, Borrelli E, Ip M, Sadda SR. Choriocapillaris flow impairment surrounding geographic atrophy correlates with disease progression. *PLoS One*. 2019;14(2):e0212563.
16. Shi Y, Zhang Q, Zhou H, et al. Correlations between choriocapillaris and choroidal measurements and the growth of geographic atrophy using swept source OCT imaging. *Am J Ophthalmol*. 2021;224:321–331.
17. Thulliez M, Zhang Q, Shi Y, et al. Correlations between choriocapillaris flow deficits around geographic atrophy and enlargement rates based on swept-source OCT imaging. *Ophthalmol Retina*. 2019;3(6):478–488.
18. Mrejen S, Spaide RF. Optical coherence tomography: Imaging of the choroid and beyond. *Surv Ophthalmol*. 2013;58(5):387–429.
19. Thorell MR, Goldhardt R, Nunes RP, et al. Association between subfoveal choroidal thickness, reticular pseudodrusen, and geographic atrophy in age-related macular degeneration. *Ophthalmic Surg Lasers Imaging Retina*. 2015;46(5):513–521.
20. Lindner M, Bezatis A, Czauderna J, et al. Choroidal thickness in geographic atrophy secondary to age-related macular degeneration. *Invest Ophthalmol Vis Sci*. 2015;56(2):875–882.
21. Borrelli E, Barresi C, Berni A, et al. OCT risk factors for 2-year foveal involvement in non-treated eyes with extrafoveal geographic atrophy and AMD. *Graefes Arch Clin Exp Ophthalmol*. 2024;262(7):2101–2109. Published online February 8, 2024, doi:10.1007/s00417-024-06399-9.
22. Huang Y, Gangaputra S, Lee KE, et al. Signal quality assessment of retinal optical coherence tomography images. *Invest Ophthalmol Vis Sci*. 2012;53(4):2133–2141.
23. Sadda SRSR, Guymer R, Holz FGFG, et al. Consensus definition for atrophy associated with age-related macular degeneration on OCT: Classification of Atrophy Report 3. *Ophthalmology*. 2018;125(4):537–548. Published online 2018.
24. McLeod DS, Grebe R, Bhutto I, Merges C, Baba T, Lutty GA. Rela between RPE and choriocapillaris in age-related macular degeneration. *Invest Ophthalmol Vis Sci*. 2009;50(10):4982–4991.
25. Hariri AH, Nittala MG, Sadda SR. Quantitative characteristics of spectral-domain optical coherence tomography in corresponding areas of increased autofluorescence at the margin of geographic atrophy in patients with age-related macular degeneration. *Ophthalmic Surg Lasers Imaging Retina*. 2016;47(6):523–527.
26. Hariri AH, Tepelus TC, Akil H, Nittala MG, Sadda SR. Retinal sensitivity at the junctional zone of eyes with geographic atrophy due to age-related macular degeneration. *Am J Ophthalmol*. 2016;168:122–128.
27. Chu Z, Shi Y, Zhou X, et al. Optical coherence tomography measurements of the retinal pigment epithelium to Bruch membrane thickness around geographic atrophy correlate with growth. *Am J Ophthalmol*. 2022;236:249–260.
28. Zhang Q, Shi Y, Shen M, et al. Does the outer retinal thickness around geographic atrophy represent another clinical biomarker for predicting growth? *Am J Ophthalmol*. 2022;244:79–87.
29. Coulibaly LM, Reiter GS, Fuchs P, et al. Progression dynamics of early versus later stage atrophic lesions in nonneovascular age-related macular degeneration using quantitative OCT biomarker segmentation. *Ophthalmol Retina*. 2023;7(9):762–770.
30. Brinks J, van Dijk EHC, Klaassen I, et al. Exploring the choroidal vascular labyrinth and its molecular and structural roles in health and disease. *Prog Retin Eye Res*. 2022;87:100994.
31. Bhutto IA, Baba T, Merges C, McLeod DS, Lutty GA. Low nitric oxide synthases (NOSs) in eyes with age-related macular degeneration (AMD). *Exp Eye Res*. 2010;90(1):155–167.

Investigative Ophthalmology & Visual Science